Rare Metal Materials and Engineering
Volume 46, Issue 9, September 2017
Online English edition of the Chinese language journal

Cite this article as: Rare Metal Materials and Engineering, 2017, 46(9): 2345-2351.

ARTICLE

Improving Al Wettability on B_4C by Transition Metal Doping: a Combined DFT and Experiment Study

Wang Zhixuan[1], Li Qiulin[2], Zheng Jiyun[2], Liu Wei[1], Shu Guogang[3], Wu Ping[4], Xu Ben[1]

[1] Tsinghua University, Beijing 100084, China; [2] Tsinghua University Graduate School, Tsinghua University City Park, Shenzhen 518055, China; [3] China Nuclear Power Engineering Co., Ltd, Technology Building, Shenzhen 518055, China; [4] Singapore University of Technology and Design, Singapore 487372, Singapore

Abstract: B_4C/Al MMC is one of the most potential neutron-shielding materials. The poor wettability of B_4C/Al interface damages the mechanical properties. To understand the alloying (or doping) effects in improving the wettability of B_4C/Al interfaces, we investigated the Al(111)/AlB_2(0001) and Al(111)/TiB_2(0001) interfacial structures via a combined approach of experiment and DFT calculations. We find a larger work of adhesion (W_{ad}) on the Al(111)/TiB_2(0001) than the Al(111)/AlB_2(0001) interfaces. The subsequently calculated partial density of states (PDOS) of doped-diborides show fewer anti-bonding states in Al(111)/TiB_2(0001) than in Al(111)/AlB_2(0001), which contribute to a stronger bonding between Ti-3d and B-2p states and lead to a higher W_{ad} and better wetting. Furthermore, we predict improved wettability of Al/B_4C by V-doping, because of the fewer anti-bonding states in vanadium-boron molecular orbitals. The same approach developed in this study may be applied for general design of alloy elements to improve the interfacial wetting of alloy-semiconductor systems.

Key words: B_4C/Al; DFT; wettability; work of adhesion; PDOS

Al-B_4C metal matrix composites are considered to be new advanced materials for the nuclear industry, primarily because of their excellent ability to capture neutrons as well as their high stiffness, high thermal conductivity and low density [1,2]. However, the poor wettability of the metal-ceramic interfaces significantly damages the mechanical properties of stir-cast Al-B_4C MMCs [3,4]. Thus it is significant to solve the wetting problem and understand the wetting mechanism.

Zhang et al. [5] found that Al-Ti alloy and Kennedy et al.[6,7] also found that K_2TiF_6 flux doped into the liquid aluminum could increase the wettability of B_4C/Al interfaces. Rajan et al. [8,9] found that B_4C particles preheated at 250 ℃ for 2 h or B_4C particles coated by copper also could improve the poor wettability between B_4C particles and Al matrix. Adding Al-Ti alloy into liquid Al to enhance the wetting is widely used in industry. But few studies have been performed to explain how Ti doping increases the wettability of the B_4C/Al interfaces.

It was demonstrated that the interface reaction products were AlB_2 and Al_3BC at 750 ℃ and that AlB_2 crystals were adjacent to the Al matrix in the work of Zhang et al.[5]. Furthermore, Zhang et al. [5,10,11] also proved that Ti introduced into liquid Al could produce Al_3BC and a new product TiB_2, which replaced AlB_2 crystals and remained to be adjacent to Al matrix. It is noticed that the diborides (AlB_2/TiB_2) remained in direct proximity to Al matrix whether doping Ti or not. This work raised an assumption that the wetting difference between Al/AlB_2 and Al/TiB_2 could be one of the reasons that affect the wettability of B_4C/Al interface. In order to validate this assumption, a stir casting experiment would be necessary to confirm that TiB_2

Received date: August 13, 2016
Foundation item: National Natural Science Foundation of China (51301094)
Corresponding author: Xu Ben, Ph. D., Associate Professor, School of Materials Science and Engineering, Tsinghua University, Beijing 100084, P. R. China, Tel: 0086-10-62772852, E-mail: xuben@mail.tsinghua.edu.cn

do replace AlB_2 and do remain in direct proximity to the Al matrix.

1 Experiment

The material used in this experiment was commercially pure aluminum (1060) reinforced with 31 wt% B_4C particles (average size ranging from 18~23 μm), containing 3.5 wt% Ti. The stirring action was performed in a vacuum mixer furnace (550 r/min) at 730 ℃. Fig.1 shows the SEM micrograph of the composite samples after a 15 min holding period. It is evident that the old AlB_2 product disappeared and was replaced by TiB_2 crystals, which continuously enclosed Al_3BC layer and were located near to the Al matrix. These agreed well with the findings of earlier reports in the work of Chen et al.[5,12] and provided a logic premise for the assumption above. Then the difference of the wettability between Al/AlB_2 and Al/TiB_2 interfaces would be studied by calculation methods.

2 Calculation Methods

Recently, the first-principles methods based on density functional theory (DFT) have been successfully applied to the detailed studies of metal/ceramic interface adhesion[13-18]. First-principles calculations can accurately provide the detailed atomic, electronic structures of the interface and quantitatively predict the work of adhesion (W_{ad}). In this work, we studied the Al/AlB_2 and Al/TiB_2 interface structures and discussed the wetting improvement of Ti element on the Al/B_4C interface.

Few experimental studies have been performed to find out the match planes between Al/AlB_2 and Al/TiB_2 interfaces. In this work, the orientation relationships between Al, AlB_2 and TiB_2 phases were chosen as:

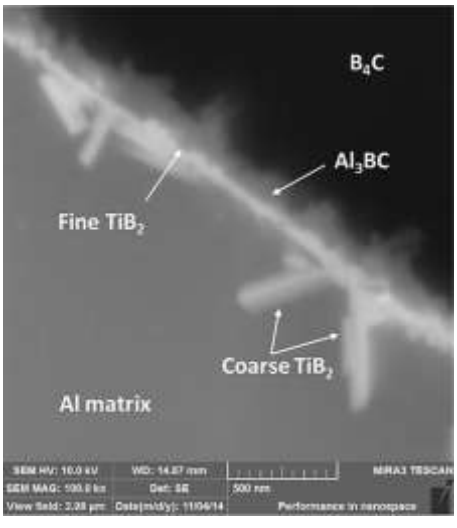

Fig.1 SEM micrograph of the Al composite containing 3.5 wt% Ti, showing the TiB_2 layers in the B_4C/Al interface (15 min holding time at 730 ℃)

$$(111)_{Al} /\!/ (0001)_{AlB_2},\ (111)_{Al} /\!/ (0001)_{TiB_2} \quad (1)$$

It is based on two reasons: 1) the close packed planes could theoretically become the match planes. Al phase is fcc structure, whose close packed plane is (111) plane; AlB_2 and TiB_2 are hcp structures, whose close packed planes are (0001) planes. The relatively small misfits between Al(111)/AlB_2(0001) and Al(111)/TiB_2(0001) are beneficial to match. 2) Zhang et al. [19] found that Al(111) matched AlB_2(0001)/TiB_2(0001) relatively well with an edge-to-edge matching model.

2.1 Bulk properties

For this study, first-principles calculations were performed with the Vienna Ab initio Simulation Package (VASP) using a plane-wave basis set for the expansion of the single-particle Kohn-Sham wave functions, and the electron-ion interaction was described using the projector-augmented-wave (PAW) method [20]. The exchange-correlation energy was described by the generalized gradient approximation of Perdew and Wang (PW91) [21]. The lattice parameter optimization calculation used a 13×13×13 Gamma *k*-mesh for Brillouin zone integrations. The calculations of the work of adhesion (W_{ad}) of Al/AlB_2 used a 8×5×1 and a 9×5×1 Gamma *k*-mesh for Al-terminated and B-terminated models, respectively. The calculations of the W_{ad} of Al/TiB_2 used the 8×5×1 Gamma *k*-mesh for Ti-/B-terminated models. All calculations employed a high plane-wave energy cutoff of 450 eV. This set of parameters assured the convergence tolerance of energy of 10^{-4} eV/atom and the Hellmann-Feynman force on atom of 10^{-3} eV/0.1 nm per atom when calculating the W_{ad} of Al/AlB_2 and Al/TiB_2 interface structures. A 1 nm of vacuum was sufficient for convergence tests and interface energy calculations.

The calculated lattice parameters of Al bulk are: $a=b=c$=0.405 nm, which are consistent with the experimental result, 0.404 nm and other theoretical results [14-16]. For the AlB_2 and TiB_2 phases with a space group symmetry P6/mmm, the lattice parameters attained by bulk calculations are $a=b$=0.301 nm and c=0.326 nm (c/a=1.08), $a=b$=0.303 nm and c=0.323 nm (c/a=1.07), respectively, which agrees well with experimental and other calculation results [22-25].

2.2 Convergence tests

The purpose of this convergence tests is to simulate the interface between the bulk-like slabs. Therefore, it is necessary to insure that all the slabs are sufficiently thick to exhibit the bulk-like interiors. In this study, we have conducted convergence tests on the Al(111), AlB_2(0001) and TiB_2(0001) slabs. Because of the polarity of the AlB_2 (0001) and TiB_2 (0001) surfaces, it is necessary to use the symmetric AlB_2 (0001) and TiB_2 (0001) slabs to eliminate the dipole effect.

With the method proposed by Boettger et al. [15,16,26], we obtained the surface energies of Al (111), AlB_2 (0001) and TiB_2 (0001) slabs, σ^N. For example, the Al (111) slabs have a surface energy of:

$$\sigma^N = \left(E^{\text{slab}} - ME^{\text{bulk}}\right)/2A \quad (2)$$

where, E^{slab} is the total energy of a relaxed slab, E^{bulk} is the chemical potentials of bulk Al, M is the number of Al atoms in the Al(111) slabs, N is the number of layers of the relaxed slab, and A is the surface area. The surface free energies of Al (111) slabs with more than five layers converge to 0.77 J/m^2, which is in agreement with the experimental value, 0.82 J/m^2 [27]. AlB_2 (0001) slabs with more than eleven layers converge to 0.94 J/m^2 (Al-terminated) and 1.51 J/m^2 (B-terminated), and TiB_2 (0001) slabs with more than eleven layers converge to 2.21 J/m^2 (Ti-terminated) and 6.05 J/m^2 (B-terminated) [28]. It should be noticed that the surface free energies of the B-terminated surfaces are larger than those of the Al-terminated and Ti-terminated surfaces, which implies that the Al-terminated and Ti-terminated surfaces are more stable than the B-terminated surface. Thus, a five-layer Al(111) slab, an eleven-layer AlB_2(0001) slab and an eleven-layer TiB_2(0001) slab are thick enough to ensure a bulk-like interior interface.

2.3 Stability

Because symmetric slabs are employed in the convergence tests, the AlB_2(0001)/TiB_2(0001) slabs in the calculations are non-stoichiometric slabs. It should be necessary to account for the effects of non-stoichiometry when calculating the surface energies of the AlB_2 (0001) and TiB_2 (0001) surfaces. The surface free energy (σ) can be defined as, taking the Al(111)/AlB_2(0001) interface as an example:

$$\sigma_{\text{AlB}_2(0001)} = \left(E^{\text{slab}} - N_{\text{Al}} \cdot \mu_{\text{Al}}^{\text{slab}} - N_{\text{B}} \cdot \mu_{\text{B}}^{\text{slab}} + PV - TS\right)/2A_{\text{surface}} \quad (3)$$

here, A_{surface} is the surface area, E^{slab} is the total energy of a fully relaxed eleven-layer AlB_2 (0001) supercell, N_{Al} and N_{B} are the numbers of the Al and B atoms in the supercell, respectively; $\mu_{\text{Al}}^{\text{slab}}$ and $\mu_{\text{B}}^{\text{slab}}$ are the chemical potentials of Al and B in the slab, respectively; P, V, T and S denote the pressure, volume, temperature and entropy of the system, respectively. The terms of PV and TS may be neglected at 0 K and typical pressures. Thus, Eq. (3) can be rewritten as:

$$\sigma_{\text{AlB}_2(0001)} = \left[E^{\text{slab}} - \left(N_{\text{Al}} - \frac{1}{2}N_B\right) \cdot \mu_{\text{Al}}^{\text{slab}} - \frac{1}{2}N_{\text{B}} \cdot \mu_{\text{AlB}_2}^{\text{bulk}}\right]/2A_{\text{surface}} \quad (4)$$

Moreover, the chemical potential of the bulk AlB_2 ($\mu_{\text{AlB}_2}^{\text{bulk}}$) is related to their 0 K heat of formation ($\Delta H_{\text{f}}^{\Theta}$) and the chemical potential of Al and B in their bulks ($\mu_{\text{Al}}^{\text{bulk}}$, $\mu_{\text{B}}^{\text{bulk}}$), which is shown as [16]:

$$\mu_{\text{AlB}_2}^{\text{bulk}} = \mu_{\text{Al}}^{\text{bulk}} + 2\mu_{\text{B}}^{\text{bulk}} + \Delta_{\text{f}}H_{\text{AlB}_2}^{\Theta} \quad (5)$$

$$\mu_{\text{AlB}_2}^{\text{bulk}} = \mu_{\text{Al}}^{\text{slab}} + 2\mu_{\text{B}}^{\text{slab}} \quad (6)$$

where, $\Delta_{\text{f}}H_{\text{AlB}_2}^{\Theta}$ is the heat of formation of AlB_2, and it can be defined as:

$$\Delta_{\text{f}}H_{\text{AlB}_2}^{\Theta} = \mu_{\text{AlB}_2}^{\text{bulk}} - \left(\mu_{\text{Al}}^{\text{bulk}} + 2\mu_{\text{B}}^{\text{bulk}}\right) \quad (7)$$

Combining Eq. (5) with Eq. (6), the following relation can be given:

$$\mu_{\text{Al}}^{\text{slab}} - \mu_{\text{Al}}^{\text{bulk}} = 2\mu_{\text{B}}^{\text{bulk}} - 2\mu_{\text{B}}^{\text{slab}} + \Delta_{\text{f}}H_{\text{AlB}_2}^{\Theta} \quad (8)$$

As is known, the chemical potentials of Al and B in the slab must be less than those atoms in their bulks. Otherwise, the compound slab would be unstable and decompose into elementary substances. Thus, the range of Al chemical potential is:

$$\Delta_{\text{f}}H_{\text{AlB}_2}^{\Theta} \le \mu_{\text{Al}}^{\text{slab}} - \mu_{\text{Al}}^{\text{bulk}} \le 0 \quad (9)$$

As shown in Fig.2a, which plots the surface energies of AlB_2 (0001) versus the Al chemical potential, the range of $\mu_{\text{Al}}^{\text{slab}} - \mu_{\text{Al}}^{\text{bulk}}$ is –0.13~0 eV, which is close to another calculation result of –0.11~0 eV [29]. The Al-terminated surface energy is much lower than that for the B-terminated surface energy over the entire Al chemical potential, indicating that the outmost atomic layer of the AlB_2 particles prefers Al to B atom termination in equilibrium conditions. In Fig.2b,

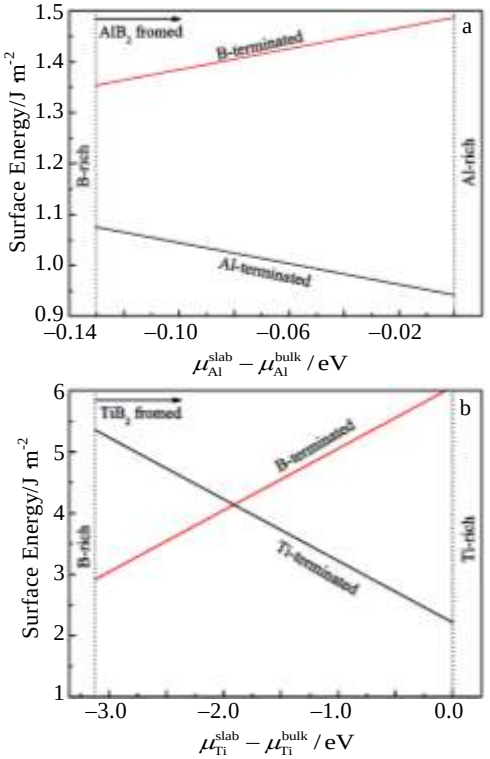

Fig.2 Relationships between the surface energies and metal chemical potentials: (a) Al- and B-terminated AlB_2(0001); (b) Ti- and B-terminated TiB_2(0001) (the vertical dash dotted lines indicate the ultimate Al and Ti chemical potential values for which bulk AlB_2 and TiB_2 form)

which shows the surface energies of TiB_2(0001) versus Ti chemical potential, the range of $\mu_{Ti}^{slab}-\mu_{Ti}^{bulk}$ is –3.12~0 eV, which agrees with the experimental value of –3.4~0 eV [30] and theoretical value of –3.2 eV [31]. The B-terminated surface is more stable than the Ti-terminated surface at low Ti chemical potential, but when the Ti chemical potential increases, the situation is reversed.

2.4 Work of adhesion and contact angles

The Al(111)/AlB_2(0001) and Al(111)/TiB_2(0001) models used the superlattice geometry in which eleven-layer AlB_2/TiB_2(0001) slab were respectively placed between two five-layer slabs of Al(111) slabs, resulting in two identical interfaces (shown in Fig. 3). To compensate for the mismatch between Al and AlB_2/TiB_2 surfaces and to satisfy the periodic boundary conditions in the supercell calculations, the (softer) Al slabs were stretched by 4.81% to be commensurated with the AlB_2 slab, and with the TiB_2 slab were stretched by 5.59%. During the geometry optimization, all atoms were allowed to be freely relaxed in three directions.

The work of adhesion (W_{ad}) can be defined as the reversible work associated with creating the respective free surfaces from a bonded interface. First-principles methods can accurately calculate the W_{ad} by determining the difference in the total energy between the interfaces; taking the Al(111)/AlB_2(0001) interface as an example:

$$W_{ad}=\left(E_{Al}^{total}+E_{AlB_2}^{total}-E_{Al/AlB_2}^{total}\right)/A_{surface} \quad (10)$$

where, E_{Al}^{total}, $E_{AlB_2}^{total}$ and E_{Al/AlB_2}^{total} are the total energy of the relaxed Al slab, AlB_2 slab and Al/AlB_2 interface, respectively, and $A_{surface}$ is the interface area. The calculated values of W_{ad} for the Al/AlB_2 and Al/TiB_2 interface structures are listed in Table 1.

In Table 1, it should be noted that for the Al/AlB_2 interface, the W_{ad} of the Al-terminated interface, 0.85 J/m^2, is smaller than that for the B-terminated interface, 1.66 J/m^2. For the Al/TiB_2 interface, the W_{ad} of the Ti-terminated is 3.06 J/m^2, larger than that for the B-terminated interface, 2.48 J/m^2. Although our calculation were performed at 0 K, it has been shown that the calculated results are valid for T > 0 K for the acceptable total-energy difference in solids[15,16,21]. In conclusion, the W_{ad} of the Ti-terminated interface is the largest of all systems studied.

Moreover, W_{ad} can be used to quantitatively predict the wetting properties of an interface:

$$W_{ad}=\gamma_{mv}+\gamma_{cv}-\gamma_{mc} \quad (11)$$

where, γ_{mv} and γ_{cv} are the surface energies of metal and ceramic, respectively, and γ_{mc} is the interfacial energy between metal and ceramic. Based on Eq.(11) and the Young relationship, we can obtain the relationship between W_{ad} and the contact angle:

$$W_{ad}=\gamma_{mv}\cdot(1+\cos\theta) \quad (12)$$

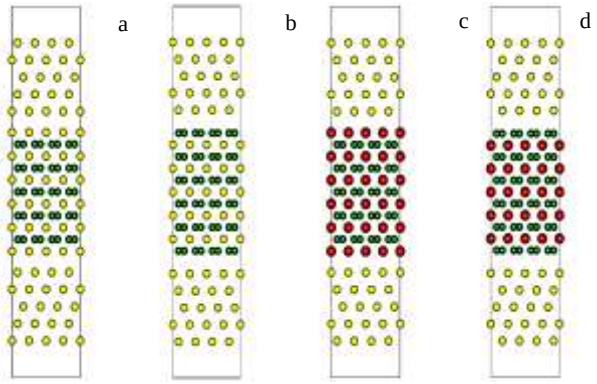

Fig.3 Al(111)/AlB_2(0001) and Al(111)/TiB_2(0001) slab models: (a) Al-terminated model for Al/AlB_2 slab, (b) B-terminated model for Al/AlB_2 slab, (c) Ti-terminated model for Al/TiB_2 slab, and (d) B-terminated model for Al/TiB_2 slab (yellow balls are Al, green balls are B and red balls are Ti)

Table 1 Values of adhesion work for Al(111)/AlB_2(0001) and Al(111)/TiB_2(0001) interfaces

Interface	Termination	W_{ad}/J m^{-2}
Al/AlB_2	Al	0.85
	B	1.66
Al/TiB_2	Ti	3.06
	B	2.48

With Eq.(12), we can easily understand that larger W_{ad} corresponds to a smaller contact angle, which means a better wettability. Comparing W_{ad} of Al(111)/TiB_2(0001) with that for Al(111)/AlB_2(0001), W_{ad} of either the Ti-terminated or B-terminated system with Al(111)/TiB_2(0001) is much larger than that of the Al-terminated or B-terminated system with Al(111)/AlB_2(0001), indicating that the Al wets better on the TiB_2 system than the AlB_2 system, with the same γ_{mv}. At this point, the assumption that the wetting difference between Al/AlB_2 and Al/TiB_2 interfaces could affect the wettability of B_4C/Al interface could be proved. This is how Ti increases the wettability of the B_4C/Al interfaces. There is no doubt that the rotation of slabs, the stacking sequences for the Al/AlB_2 and Al/TiB_2 interfaces could be other factors to affect the wettability of B_4C/Al interface.

3 Discussion

3.1 PDOS of AlB_2 and Ti-AlB_2 systems

We concluded that it is the stronger bonding formed between Al-TiB_2 that may result in the larger W_{ad} and enhance the wettability. Therefore, we selected the partial density of states (PDOS) of Me-B atoms to reveal the formation mechanism of the bonds between Al, Ti and B. In the calculation, a 2×2×2 AlB_2 supercell was adopted. In the doped

system, the Al atom at the spatial center of the supercell was replaced by a Ti atom.

The PDOS by atom of AlB_2 and Ti-AlB_2 are shown in Fig.4. The overlaps between the B-2s and B-2p states in AlB_2 and Ti-AlB_2 indicate the sp2 hybridization, which form the main bonding among boron layers. For the Ti-AlB_2 system, the energy range of the PDOS is obviously narrower than that of the PDOS of AlB_2. Moreover, the PDOS of Al shows a high peak of the 3s states and residuals 3p states around the Fermi level. In addition, the Ti-4s and Ti-3p states are mainly localized and contribute little to the bonding states. However, there are two peaks around the Fermi energy in the PDOS of Ti-B (Fig. 4b-IV). The one below the Fermi level (-2.4 eV) is a result of the hybridization of Ti-3d and B-2p states, which contributes to Ti-B covalent bonds. The other peak above the Fermi level (0.8 eV) consists of the hybridization of Ti-3d states and Al-3s states, which results in Ti-Al metallic bonds. The hybridization among Ti-3d, Al-2s and B-2p contribute to a steep pseudogap at the Fermi energy in the PDOS of Ti-AlB_2 instead of a more "flat" pseudogap for AlB_2. The intensified anti-bonding states above the Fermi energy of AlB_2, which indicates more anti-bonding states, result in less stable Al-B bonds, comparing with the Ti-B bonds. Accordingly, we could draw a clear conclusion as to the reason that Al wets TiB_2 better than AlB_2. As a result of electron transfer, no extra electrons of TiB_2 enter the anti-bonding space, which stabilizes the cohesion between Ti-3d and B-2p. Thus, stronger bonds can contribute to large W_{ad} and lower contact angles to achieve a better wettability.

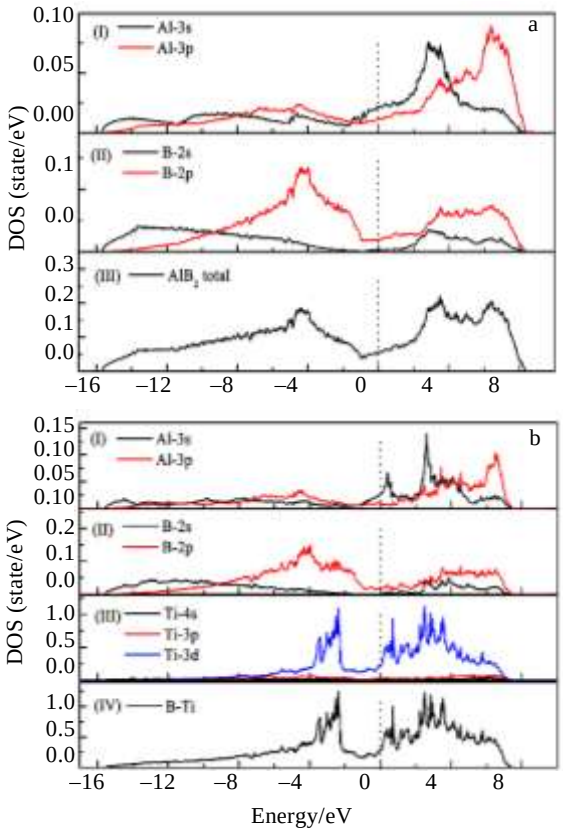

Fig.4 Partial density of states of AlB_2 and Ti-AlB_2 systems: (a) partial Al, B density of states and total density of states of AlB_2; (b) partial Al, B, Ti density of states and total density of states of Ti-AlB_2 (the vertical lines indicate the Fermi level E_F)

3.2 PDOS of Me-AlB_2 systems

As previous papers reported, Ti is widely used in industry to improve the wettability of the Al/B_4C system, but it performs badly at low temperatures of approximately 700~900 ℃. Therefore, it is important to find more ideal alloy elements to increase the wettability of the Al/B_4C system. Taking the elements with similar chemical properties into consideration, we choose Sc, V, Y, Zr and Nb as candidates. On the other hand, commercially pure Al contains many dopants such as Mg and Cr. which may damage the wettability of the Al/B_4C system. It is therefore necessary to study the wetting influence of the dopants. The PDOS curves of the supercells are shown in Fig.5 after replacing the Al atom at the spatial center of a 2×2×2 AlB_2 supercell by a dopant (Sc, V, Cr, Y, Zr, Nb).

It is found that the PDOS of Sc-, Y-, Zr- and Nb-AlB_2 are almost zero and cannot contribute to the Me-B bonding nor lower the contact angles. Comparing the PDOS of residual V-, Cr-AlB_2 and AlB_2, we find that the hybridization of B-2s and B-2p are still the dominant bonding states among boron layers and that the energy ranges of PDOS are also shorter than AlB_2. For V-AlB_2, there are still two peaks around the Fermi level in the PDOS of V-B. One peak below the Fermi level is a result of the hybridization of V-3d and B-2p states, which indicates covalent bonds between V and B. The other peak above the Fermi level consists of the hybridization of V-3d and Al-3s states, which shows the metallic bonds. These two peaks form a steep pseudogap at the Fermi energy. The weaker anti-bonding states of the V-B PDOS compared to the AlB_2 PDOS could stabilize the V-B bonds, which may lower the contact angles between Al phase and VB_2 phase. A peak at the Fermi level in the B-Cr PDOS is formed by the hybridization of Al-3s and Cr-3d states, indicating the formation of Al-Cr metallic bonds. Moreover, there are two peaks below the Fermi level, which consist of Al-3d, B-2p and Cr-3d states. The fact that the anti-bonding states form a peak at the Fermi level indicates more anti-bonding states compared with AlB_2, which could weaken the bonding among Al, B and Cr, and damage the wettability of Al and CrB_2 to be even worse than Al and AlB_2.

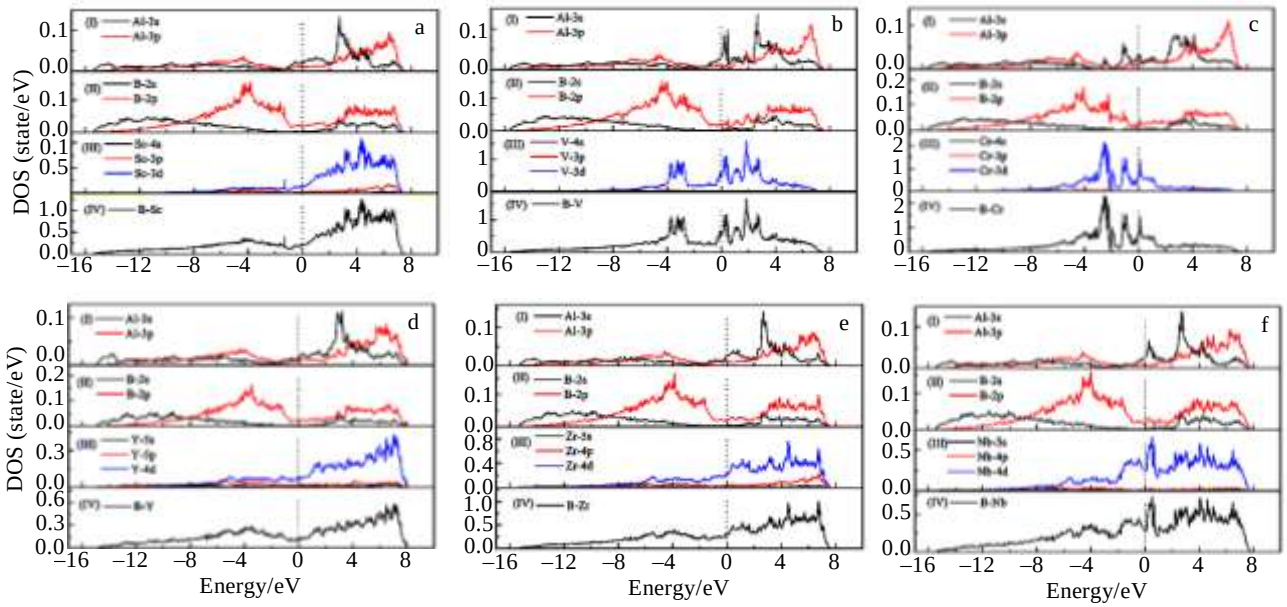

Fig.5 Partial density of states of Me-AlB_2 systems: (a) the Sc-doped AlB_2 system, (b) the V-doped AlB_2 system, (c) the Cr-doped AlB_2 system, (d) the Y-doped AlB_2 system, (e) the Zr-doped AlB_2 system, and (f) the Nb-doped AlB_2 system (the vertical lines indicate the Fermi level E_F)

4 Conclusions

1) The Al(111)/TiB_2(0001) interface has higher adhesion energies than the Al(111)/AlB_2(0001) interface, which means the Al(111)/TiB_2(0001) interface has a better wettability. The wetting difference between Al matrix and diborides is one of the factors to influence the wettability of B_4C/Al interfaces.

2) For AlB_2(0001), the Al-terminated surface is more stable than the B-terminated surface, but the surface stability relationship of TiB_2(0001) is dominated by the Ti chemical potential.

3) It is evident that the stronger bonding of the Al/TiB_2 over the Al/AlB_2 interface is a result of the fewer anti-bonding states with electron transfer. The more stable bonding achieves the larger W_{ad} for the Al/TiB_2 interface, which indicates a better wettability. Thus the reason why the wettability of Al-B_4C MMCs could be improved with Al-Ti alloy addition is proved.

4) The PDOS of V-doped AlB_2 shows fewer anti-bonding states than AlB_2; thus, Al-V alloys may also improve the wettability of the Al/B_4C interface and may be promising candidates for industrial applications.

References

1 Kim S, Sachdev A K. In Yin W, Das S K eds. *Aluminum Alloys: Fabrication, Characterization, and Applications*[M]. Warrendale, PA: TMS, 2008: 51

2 Viala J C, Bouix J, Gonzalez G *et al. Journal of Materials Science*[J], 1997, 32: 4559

3 Delannay F, Froyen L and Deruyttere A. *Journal of Materials Science*[J], 1987, 22: 1

4 Halverson D C, Pyzik A J *et al. Journal of the American Ceramic Society*[J], 1989, 72: 775

5 Zhang Z, Fortin K, Charette A *et al. Journal of Materials Science*[J], 2011. 46: 3176

6 Kennedy A R. *Journal of Materials Science*[J], 2002, 37: 317

7 Kennedy A R, Brampton B. *Scripta Materialia*[J], 2001, 44: 1077

8 Deepa J P, Resmi V G, Rajan T *et al. T Indian I Metals*[J], 2011, 64: 47

9 Mahesh V P, Nair P S, Rajan T *et al. Journal of Composite Materials*[J], 2011, 511: 089 026

10 Zhang Z, Chen X G, Charette A. *Journal of Materials Science*[J], 2009, 44: 492

11 Zhang Z, Chen X G, Charette A. *Journal of Materials Science*[J], 2007, 42: 7354

12 Lai J, Zhang Z, Chen X G. *Journal of Materials Science*[J], 2011, 46: 451

13 Li Y, Gao Y, Xiao B, Ma S *et al. Applied Surface Science*[J], 2011, 257: 5671

14 Liu L M, Wang S Q, Ye H Q. *Acta Materialia*[J], 2004, 52: 3681

15 Siegel D J, Hector L G *et al. Physical Review B*[J], 2003, 67: 92105

16 Siegel D J, Hector L G *et al. Surface Science*[J], 2002, 498: 321

17 Zhang W, Smith J R. *Physical Review B*[J], 2000, 61: 16 883

18 Shu G G, Xu Q, Wu P. *ACS Applied Materials & Interfaces*[J], 2015, 14: 7576

19 Zhang M, Kelly P M *et al*. *Acta Materialia*[J], 2005, 53: 1427
20 Kresse G, Joubert D. *Physical Review B*[J], 1999, 59: 1758
21 Perdew J P, Chevary J A *et al*. *Physical Review B*[J], 1992, 46: 6671
22 Burdett J K, Canadell E, Miller G *J*. *Journal of American Chemical Society*[J], 1986, 108: 6561
23 Lie K, Høier R, Brydson R. *Physical Review B*[J], 2000, 61: 1786
24 Loa I, Kunc K, Syassen K *et al*. *Physical Review B*[J], 2002, 66: 134 101
25 Tian D, Wang X. *Journal of Physics-Condensed Matter*[J], 1992, 4: 8765
26 Boettger J C. *Physical Review B*[J], 1994, 49: 16 798
27 Tyson W R, Miller W A. *Surface Science*[J], 1977, 62: 267
28 Han Y F, Dai Y, Shu D *et al*. *Journal of Physics-Condensed Matter*[J], 2006, 18: 4197
29 Han Y F, Dai Y B *et al*. *Applied Surface Science*[J], 2011, 257: 7831
30 Topor L, Kleppa O J. *The Journal of Chemical Thermodynamics*[J], 1985, 17: 1003
31 Han Y F, Dai Y B, Shu D *et al*. *Applied Physics Letters*[J], 2006, 89: 144 107

过渡元素改善 B_4C/Al 材料界面润湿性的机理研究

王治璇[1]，李丘林[2]，郑继云[2]，刘　伟[1]，束国刚[3]，吴　平[4]，徐　贲[1]

(1. 清华大学，北京 100084)

(2. 清华大学深圳研究生院，广东 深圳 518055)

(3. 中国核电工程有限公司，广东 深圳 518055)

(4. 新加坡科技设计大学，新加坡 487372)

摘　要：B_4C/Al复合材料是目前最理想的中子吸收材料，但工业上常用的液态搅拌法制备过程中存在着界面润湿性差的问题。结合实验及第一性原理的方法，通过研究Al(111)/AlB_2(0001)和Al(111)/TiB_2(0001)界面的结构来分析工业上添加过渡元素Ti对B_4C/Al界面润湿性的改善机制。通过计算发现，Al(111)/TiB_2(0001)界面相对Al(111)/AlB_2(0001)界面具有更高的粘附功值，说明其界面结合更强。进一步对比Ti掺杂二硼化物和AlB_2的偏态密度结构，发现Ti掺杂体具有较低的反键态，表明Ti-3d和B-2p轨道电子杂化后，在B、Ti原子间形成了较强的化学键，从而促进了Al(111)/TiB_2(0001)界面处的强结合作用，提高了Al(111)/TiB_2(0001)界面粘附功，故而改善了B_4C/Al界面的润湿性。根据同样的理论依据，V掺杂体也具有较低的反键态，V和B之间的强结合效果或许能够改善B_4C/Al界面的润湿性，成为又一理想的溶体改性掺杂元素。

关键词：碳化硼铝基复合材料；密度泛函理论；润湿性；粘附功；偏态密度

作者简介：王治璇，女，1989 年生，硕士，清华大学材料学院，北京 100084，电话：010-62772852，E-mail: 961695557@qq.com